Grenze International Journal of Engineering and Technology, January Issue

Improvement of Propulsive Efficiency of a Tandem Aerofoil Following Fishtailed Motion

Dr. Prafulla Kumar Swain[1] and Dr. Anitha Guttavelli[2]
[1-2]GITAM Deemed to be University/Dept. of Mechanical Engineering, Visakhapatnam, India
Email: kprafull@gitam.edu, aguttave@gitam.edu

***Abstract*—To enhance performance in both aerial and aquatic locomotion, many bird flocks and fish schools adopt a tandem arrangement of wings or fins. Recent studies in this field, particularly those involving fluttering foils, remain challenging due to their complex flow dynamics. In this work, the focus shifts from the conventional flapping pattern characterized by vertical heave and pitch motions to a novel fishtail flapping trajectory for tandem hydrofoils. The foil motion is simulated using an ALE framework in conjunction with a dynamic mesh, allowing the incompressible Navier–Stokes equations to be solved for the surrounding flow field. Alongside trajectory analysis, the effects of Strouhal number (St) and foil phase angle (φ) on thrust generation are examined. Findings indicate that employing a tandem flapping foil configuration with elliptical or fishtail motion can substantially improve both thrust output and propulsive efficiency.**

***Index Terms*—fore foil, hind foil, fishtailed motion trajectory, computational fluid dynamics, propulsive efficiency.**

I. Introduction

Globally, significant research efforts have been directed toward designing autonomous underwater vehicles (AUVs) that replicate the thrust-generation strategies observed in aquatic creatures like fish. To improve the induced thrust, researchers from all over the world try to apply the motion of aquatic animals to flapping foil. According to research by Liao et al. [1] on swimming fish behind a D-section cylinder, the fish needs less effort to go forward when it passes through the vortex street than when it doesn't. A dead fish can also proceed if it passes through the vortex street, according to Beal et al. [2]. Shao et al. [3] discovered that the energy of the vortices was used to boost the induced thrust in a 2D simulation. Maertens et al. [4] investigated the vortex interactions occurring between fish positioned in a tandem arrangement, considering both in-phase and counter-phase swimming patterns. Deng et al. [5] conducted a two-dimensional simulation of a tandem flapping foil following a sinusoidal path. Swain et al. [6] and Gopal krishnan et al. [7] also report a similar outcome. Instead of using only heave and pitch motion, Xiao et al. [8] employed a trapezoidal flapping trajectory. They found that up to 50% more thrust can be produced simply altering the foil's motion. To improve induced thrust and propulsive efficiency, Ashraf.M et al. [9] and Platzer.M et al. [10] replace conventional sinusoidal motion with non-sinusoidal heaving and pitching characteristics, they found that non-sinusoidal motion has a 17% greater propulsive efficiency than sinusoidal motions.

Grenze ID: 01.GIJET.12.1.523_1

In the current work, the different positions of downstream foil in relation to upstream foil, as well as tandem flapping foil with fishtail trajectory, are investigated numerically. The research is expanded to include varying smoothing factor values that characterize the fishtailed path.

II. Materials and Methods

A. Flapping Foil Motion Characteristics

In this work, a 2-D computational model is developed using a NACA0012 foil, as depicted in Fig.1. The motion patterns of a single foil under both basic and fish-tail kinematics are illustrated in Figs. 1a and 1b, whereas Fig. 1c presents the geometric configuration of fish-tail motion in a tandem foil setup.

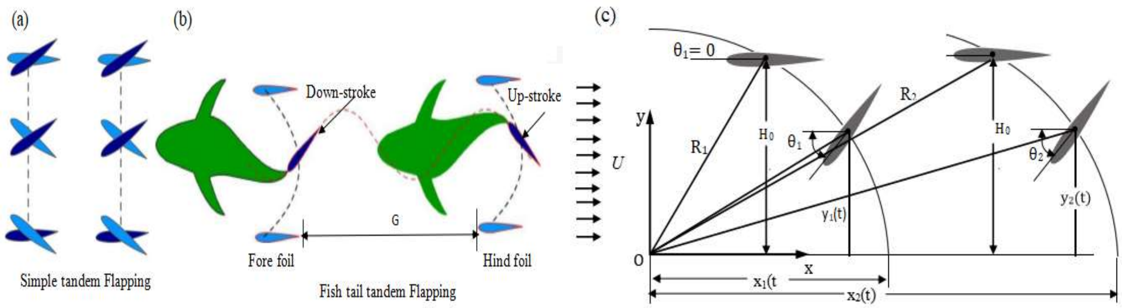

Figure 1: (a) simple flapping (b) fishtail flapping (c) the foils moving both horizontally and vertically

In the basic tandem flapping configuration, the foil performs a combination of heaving and pitching motions. In contrast, under the fish-tail mode, the foil moves in both vertical and horizontal directions. The simple flapping trajectory's pitch and heave profiles are explained by Eqs . 1 and 2.

$$H(t) = H_0 \sin(\omega t + \varphi) \tag{1}$$

$$\theta(t) = \theta_m \sin(\omega t + \varphi) \tag{2}$$

Fish tail flapping is accomplished by using Eqs 3-6 for both motions, which are derived from Fig. 2.

$$x_1(t) = R_1 \cos\left[\tan^{-1}\left(\frac{1}{(R_1/H_o) - S'}\right)\sin(\omega t)\right] \tag{3}$$

$$y_1(t) = R_1 \sin\left[\tan^{-1}\left(\frac{1}{(R_1/H_o) - S'}\right)\sin(\omega t)\right] \tag{4}$$

$$x_2(t) = R_2 \cos\left[\tan^{-1}\left(\frac{1}{(R_2/H_o) - S'}\right)\sin(\omega t)\right] \tag{5}$$

$$y_2(t) = R_2 \sin\left[\tan^{-1}\left(\frac{1}{(R_2/H_o) - S'}\right)\sin(\omega t)\right] \tag{6}$$

B. Computational Approach and Validation

Mathematical modeling

The 2-D Naiver-Stokes equations for the unstable incompressible flow over the NACA0012 foil are expressed as

$$\frac{\partial u_x}{\partial x} + \frac{\partial u_y}{\partial x} = 0 \tag{7}$$

$$\frac{\partial u_x}{\partial t} + u_x \frac{\partial u_x}{\partial x} + u_y \frac{\partial u_y}{\partial y} + \frac{1}{\rho}\frac{\partial p}{\partial x} = F_x + \mu \nabla^2 u_x \tag{8}$$

$$\frac{\partial u_y}{\partial t} + u_x \frac{\partial u_y}{\partial x} + u_y \frac{\partial u_y}{\partial y} + \frac{1}{\rho}\frac{\partial p}{\partial y} = F_y + \mu \nabla^2 u_y \tag{9}$$

where u_x and u_y denote the velocity components, Fx and Fy represent the body forces along the x-and y-directions, respectively, μ is the viscosity and p is the pressure.

Meshing and Setup

The ANSYS FLUENT design environment was used to build the geometry of the computational model. It consists of one rectangular fluid domain and two circular fluid zones encircling the aerofoils. The rectangular domain measures 0.8×0.5 meters. An overview of the complete mesh (not to scale) is presented in Fig. 2a, while Fig. 2b provides a closer view of the two circular domains containing counter-phase aerofoils. A detailed view of the finely meshed circular domain is shown in Fig. 2c. As illustrated in Fig. 2d, twenty inflation layers are applied around the hydrofoils, with an initial layer height of 1×10^{-4} m (corresponding to a y+ value of 0.005 m) and a growth rate of 0.12.

The interference wall encloses the circular fluid domain. Free/no-slip walls define the fluid domain's upper and lower bounds. The domain's opposite end is given an inlet velocity of 0.1173 m/s and the other end is kept at zero pressure. The aerofoil's flapping motion is achieved using a dynamic mesh. Equations (1) -(6), describing the two flapping trajectories, are programmed in C, and the motion is imparted to the aerofoil through a user-defined function (UDF).

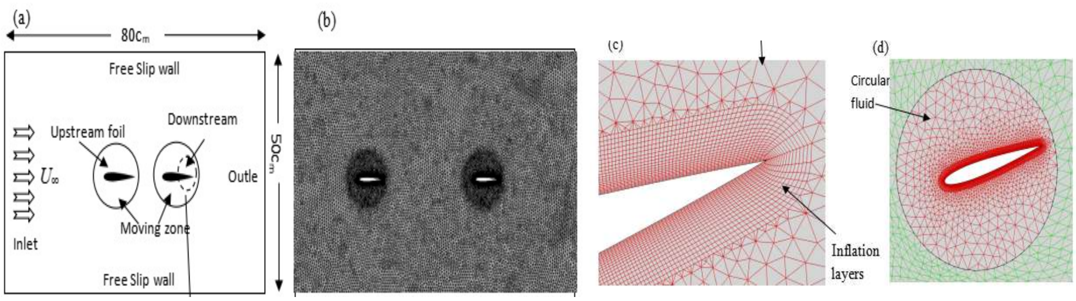

Figure 2: Computational fluid domain: (a) Full fluid domain (not to scale), (b) Circular fluid domain with extremely fine mesh, (c) Views of the fore and rear foil magnified, (d) zoomed-in image of the inflated layer.

While the rectangular fluid domain is regarded as a deforming body, the circular fluid zones and the two aerofoils are modelled as rigid bodies. Using a velocity-pressure coupling approach, the transient simulations are resolved until the thrust coefficient completely converges. The continuity and velocity equations in the computational model are solved using a coupled solution approach with a convergence tolerance of 10^{-5}.

Dimensionless parameters

Pitch and heave contributions combine to provide the impetus that the incoming flow elicits. The following a used to determine the mean thrust force, mean power, and coefficient of propulsive performance:

$$\overline{C_T} = \frac{C_T}{\frac{1}{2}\rho c U_\infty^2} \quad \text{and} \quad \overline{C_P} = \frac{P}{\frac{1}{2}\rho c U_\infty^3} \tag{10}$$

$$P_{input} = \frac{1}{T}\int_0^T \left[F_y(t)\frac{dy(t)}{dt} + F_x(t)\frac{dx(t)}{dt} + M(t)\frac{d\theta(t)}{dt} \right] dt \tag{11}$$

where $F_x(t)$ and $F_y(t)$ are the forces created in the x and y directions, respectively and M (t) is the pitch moment. Lastly, the following formula can be used to calculate the propulsive efficiency:

$$\eta = \frac{\overline{C_T}}{\overline{C_P}} \tag{12}$$

For hind foil, the propulsive efficiency η is defined. The flapping trajectory is the main subject of this investigation. Prior studies [11–13] indicates that most fish and birds cruise at *St* between 0.2 and 0.5 during swimming or flight. To achieve *St* values within this range, the present work maintains a suitable flapping frequency while also varying the flapping trajectory.

Grid Independence Analysis and Computational Method Validation

The grid and time step independence of the three grid sets (coarse, medium, and fine) have been verified. We compared the results with the computational results of Esfahan and the experimental results of Akbari and Price [12-13]. We assumed a laminar flow and used a second-order accurate upwind approach.

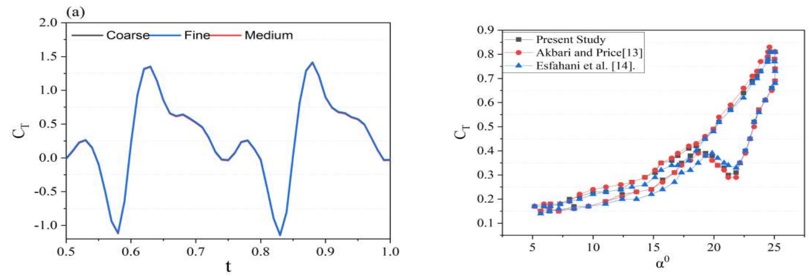

Figure 3: (a) C_T versus instantaneous time. (b) Model validation: C_T with variation of angle of attack

A second-order precise backward implicit method was used to discretise time. The time steps t = T/1000, t = 8T/1000, and t = 6T/1000 were chosen as indicated in table-2. The varying mean lift coefficients over cycle time (T) for the various gird types taken into consideration in the gird independent investigation are displayed in Fig. 3a. Fig. 3b shows the average thrust of NACA0012 foil with the *St.* The narrow fluctuation observed is due to the viscosity of the fluid.

III. Results and Discussion

A. Vortex flow generated by a single foil

To comprehend the thrust-induced process of a single flapping foil, the Z vorticity contour is used to visualize the flow surrounding the foil. Figure 4 displays the vorticity contour for both basic and fishtailed trajectories with a range of *St* between 0.2 and 0.4. The flapping frequency or *St* controls the wake created at the foil's trailing edge and a higher flapping frequency produces a closer vortex. As seen in Figure 4, the created vortex produces dipoles in a horizontal line.

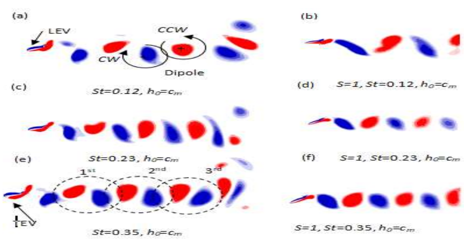

Figure 4: Z-Vorticity of a Single Foil at maximum thrust in Simple Flapping Mode- (a, c, e) and along fish tailed trajectory-(b, d, f)

The fluid contributes to the thrust generation of the flapping foil through a reactive effect, as the formation of a dipole creates a jet aligned with the direction of fluid flow. With increasing St, a greater number of dipoles are generated, thereby amplifying the induced thrust. Consequently, the spacing between successive dipoles decreases with higher St, leading to stronger interactions between vortices and dipoles at shorter separations compared to wider ones. As a result, the flapping foil performs better hydrodynamically at higher St values than at lower ones. This is evident from Table 1 and Figure 5.

TABLE I: AVERAGE THRUST COEFFICIENT VERSUS GRID ELEMENT COUNT

Parameter	No of elements	Average thrust coefficient	Percentage difference
Coarse	97000	0.27882	--
Medium	124000	0.27037	3.03
Fine	183000	0.28012	3.60

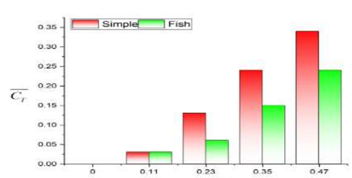

Figure 5: Thrust Coefficients of Single Foils for different St

B. Effect of Flapping trajectory on thrust generation in tandem Foils

The interplay between the vortices produced by the fore and aft foils is a crucial element influencing the amount of induced thrust in a tandem flapping foil system. Depending on factors including flapping frequency (St), flapping trajectory, and the aft foil's relative position to the fore foil, this vortex interaction can either increase or decrease the aft foil's hydrodynamic efficiency. In the current work, 60 simulations were carried out by methodically altering the phase angle, flapping trajectories, and inter-foil distance. The results of these tandem flapping configurations are summarized in Table 2.

TABLE II: 2D TANDEM SIMULATION RESULTS [H0/CM=1, S=0(SIMPLE FLAPPING), S=0.5,0.75 AND 1 (FISH TAIL TRAJECTORY)]

Case	S	St	α(deg)	ϕ	η
1	0	0.23	5	0	0.32
2	1	0.3	10	0	0.29
3	0	0.3	7	π	0.36
4	1	0.4	11	π	0.39
5	0	0.2	10	0	0.29
6	1	0.3	10	0	0.28
7	0	0.5	6	π	0.38

The wake vortices produced by the fore foil can interact with the aft foil in three different ways, according to an analysis of all the simulations carried out in this work. In the first instance, the aft foil is struck immediately by the approaching wake from the fore foil as shown in Fig. 6c for simple flapping and Fig. 6d for fish-tail flapping. In the second case, only the upper or lower portion of the incoming wake makes partial contact with the aft foil, illustrated in Fig. 6e for simple flapping and Fig. 6f for fish-tail flapping. In the third case, the aft foil oscillates between the paths of the incoming wake, as depicted in Fig. 6a for simple flapping and Fig. 6b for fish-tail flapping.

Flow visualizations of the vorticity fields around the foils reveal that the wake patterns, as well as the manner in which the upstream wake interacts with the downstream foil, differ significantly between simple and fishtail motion trajectories. These differences influence both the energy requirements and propulsive efficiency of the system. For reduced frequencies up to 0.17, the downstream foil in an elliptical tandem configuration operating in counter-phase achieves higher energy efficiency. However, at higher reduced frequencies, the trend reverses (Fig. 7a). At these higher frequencies, the wake generated at the trailing edge experiences limited deflection, resulting in fewer available flow paths for the downstream foil
to pass through the upstream wakes (Figs. 6c, d).

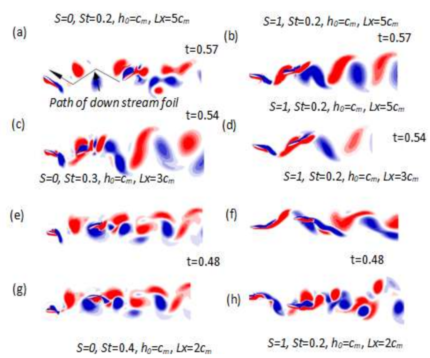

Figure 6: Z-Vorticity Characteristics of TFF in Counter-Phase Motion

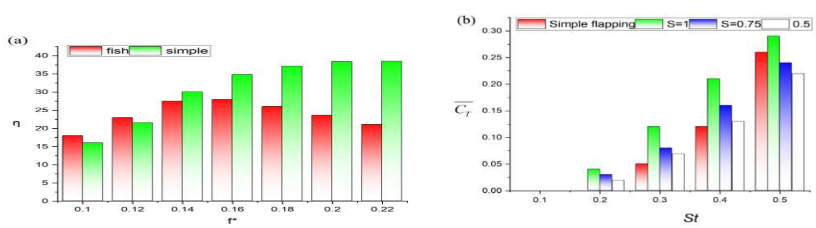

Figure 7: (a)Propulsive Performance of the DF in CPM (b)Thrust Coefficient Profiles of Single Foils at Multiple St

In contrast, at lower frequencies, the greater horizontal deflection of the wakes has a stronger influence on the downstream foil. Figures 8a-f present the wake structures produced by a tandem flapping foil executing both basic and fish-tail trajectories, with the upstream and downstream foils flapping in phase. At a frequency of 0.15 (Figs. 9a, b), the downstream foil repeatedly traverses the wake generated by the upstream foil, creating an additional dipole that boosts lift in both motion modes. However, at higher frequencies, the basic flapping mode shows superior performance compared to the fish-tail motion, as in the latter case the upstream wake directly strikes the downstream foil, leading to a reduction in lift (Figs. 8a, c, e). At higher frequencies, the trailing-edge (TE) wake generated by the upstream foil during simple flapping can form a dipole behind the downstream foil, boosting lift (Fig. 9a). However, at such frequencies, the TE wake shows limited deflection, restricting the available flow paths for the downstream foil to pass through the upstream wake (Figs. 9a, b). At lower frequencies, the wakes are deflected with larger horizontal amplitudes, allowing the downstream foil to pass through the dipole region without direct interference.

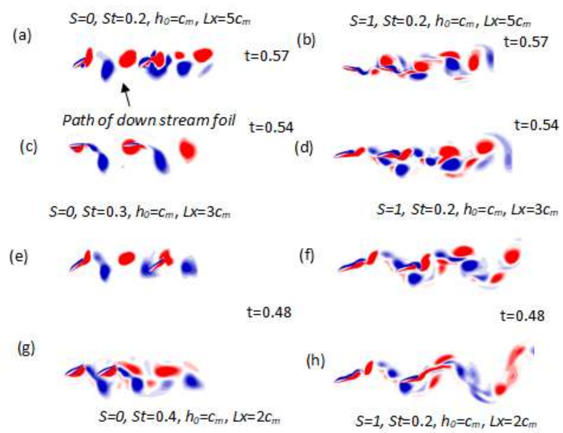

Figure 8: Z-Vorticity Analysis of Tandem Foils During In-Phase Flapping

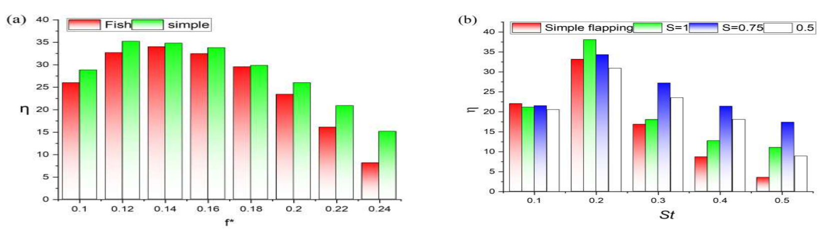

Fig 9:(a) Downstream foil's efficiency during in-phase flapping (b) Thrust coefficients at various St.

IV. CONCLUSIONS

The current study's computational model examines how the wake produced by the fore and aft foils interact when they are arranged in tandem. Two different elliptical and fishtailed flapping trajectories in a single and tandem setup by adjusting the St between 0.2 and 0.5, the flapping foil is investigated. Beyond the variations in flapping trajectories and St, the study also examines the impact of modifying the phase angle between the foils. As the wake produced at the trailing edge generates induced thrust for a single flapping and the elliptical flapping enhances thrust by creating a stronger wake between the two flapping trajectories as opposed to a fishtailed trajectory. A higher value of St increases the thrust generated during single flapping in comparison to a lower value. Lastly, the ability of a tandem flapping foil to propel is typically determined by how well the fore and aft foils work together to form a vortex.

ACKNOWLEDGMENT

This work is supported by DST NMICPS, Technology Innovation Hub for Autonomous Navigation-TiHAN, IIT Hyderabad

REFERENCES

[1] J. C. Liao, D. N. Beal, G.V. Lauder, and M.S.Triantafyllou, "Fish exploiting vortices decrease muscle activity," Science 302, 1566 (2003).

[2] D. N. Beal, F. S. Hover, M. S. Triantafyllou et al.,"Passive propulsion in vortex wakes," J. Fluid Mech. 549, 385, (2006).

[3] X. Shao, D. Pan, J. Deng, and Z. S. Yu, "Hydrodynamic performance of a fish like undulating foil in the wake of acylinder," Phys. Fluids 22(11), 111903 (2010).

[4] A. P. Maertens, A. Gao, and M. S. Triantafyllou, "Optimal undulatory swimming for a single fish-like body and for a pair of interacting swimmers, J. Fluid Mech. 813, 301 -345, (2017).

[5] J. Deng, X.-M. Shao, and Z.-S. Yu, "Hydrodynamic studies on two traveling wavy foils in tandem arrangement," Phys.Fluids 19, 113104 (2007).

[6] P. K. Swain, B.N.S.A. Challa, N.A. Ganti, S.P. Dora, AK Barik, "Effect of Flapping Trajectory and inter foil distance on Propulsive Performance of a Tandem Flapping Foil", ASME-Journal of Off sore mechanic's and artic engineering.,5(2022),1-11.

[7] R. Gopalkrishnan, M. S. Triantafyllou, G. S. Triantafyllou, and D. Barrett, "Active vorticity control in a shear flow using a flapping foil," J. Fluid Mech. 274, 1 (1994).

[8] Q. Xiao, W. Liao, S.C. Yang, Y. Peng, "How motion trajectory affects energy extraction performance of a biomimic energy generator with an oscillating foil", Renewable Energy, 37 (1) (2012) 61-75.

[9] M. A. Ashraf, J. Young and J. C. S. Lai, "Reynolds number, thickness and camber effects on flapping airfoil propulsion", Journal of Fluids and Structures, 27(2011), 145-160.

[10] M. Platzer, M. Ashraf, J. Young, J. Lai, "Development of a new oscillating-wing wind and hydropower generator", in: 47th AIAA Aerospace Sciences Meeting, 2009.

[11] Swain, P.K., Dora, S.P., "Experimental and numerical investigation of wing–wing interaction and its effect on aerodynamic force of a robotic dragonfly during hovering and forward flight", Arch Appl. Mech. 91(2021),2039-2055.

[12] Swain, P.K., Dora, S.P, Suryanarayana, M.B., Barik, .A.K, "Numerical investigation of wing-wing interaction and its effect on the aerodynamic force of a hovering dragonfly", SAGE(2021) , Journal of aerospace Engg.

[13] Akbari, MH, Price SJ. "Simulation of dynamic stall for a NACA 0012 airfoil using a vortex method", Journal of Fluids Structure, 17 (2003),855-874.